

Structure of the adatom electron band of the Si(111)-7×7 surface

J. Mysliveček,¹ A. Stróżecka,¹ J. Steffl,² P. Sobotík,² I. Ošťádal,² and B. Voigtländer^{1,*}

¹*Institut für Schichten und Grenzflächen (ISG 3), Forschungszentrum Jülich, D-52425 Jülich, Germany
and CNI-Center of Nanoelectronic Systems for Information Technology, Forschungszentrum Jülich, D-52425 Jülich, Germany*

²*Faculty of Mathematics and Physics, Department of Electronics and Vacuum Physics, Charles University, V Holešovičkách 2,
180 00 Praha 8, Czech Republic*

(Received 23 January 2006; published 11 April 2006)

We use variable temperature scanning tunneling spectroscopy to determine the space and energy structure of the adatom electron band of the Si(111)-7×7 surface. At low temperature (7 K) we map the wave functions of the electrons in the adatom band in real space. We observe a pronounced splitting of the adatom electron states between corner and center adatoms of the surface reconstruction and identify new spectral features in the unoccupied part of the adatom band. The adatom electron states are subsequently identified in tunneling spectra at room temperature to obtain their energy unaffected by electron transport limitations at low temperature.

DOI: [10.1103/PhysRevB.73.161302](https://doi.org/10.1103/PhysRevB.73.161302)

PACS number(s): 73.20.At, 68.47.Fg, 68.37.Uv, 68.37.Ef

Scanning tunneling microscopy (STM) and scanning tunneling spectroscopy (STS) played an important role in determining the structure and electronic properties of the Si(111)-7×7 surface. In seminal works, the real-space view of the Si(111)-7×7 surface¹ and the related spatially resolved surface electron spectra² were measured by STM and STS. These results, when combined with the results of other surface-sensitive techniques, provided compelling support for the dimer-adatom-stacking-fault (DAS) model of the Si(111)-7×7.³ They also provided information about the surface electronic structure comprising pronounced features assigned to back bonds, rest atoms, and adatoms of the Si(111)-7×7 surface.^{4,5}

We present a detailed variable temperature STS study of the structure of the adatom electron band of the Si(111)-7×7 surface. At low temperatures (LT), the combination of point STS measurement and spectroscopic imaging reveals new spectral features in the unoccupied part of the adatom electron band and a strong splitting of the electron states between the corner and center adatoms of the DAS structure. However, at LT the energies of the spectral features are shifted due to a limited transport of electrons between the surface and the bulk.^{6,7} We explain this effect in terms of nonequilibrium tunneling⁷ on surfaces with a high density of surface electron states. To obtain an energy scale uninfluenced by the transport limitation, we identify the spectral features and measure their energies in the point STS spectra at room temperature (RT). The combination of LT and RT spectroscopy is a powerful experimental methodology. The LT measurements have the advantage of high space and energy resolution and the RT measurements provide a true energy scale.

We performed the measurements in an ultrahigh vacuum on a commercial LT STM (Ref. 8) and a noncommercial variable temperature STM with active drift compensation.⁹ The Si(111) substrates were degenerately *n*-doped ($1.6 \times 10^{19} \text{ cm}^{-3} \text{ As}$), keeping a constant carrier density at temperatures down to 4.2 K.¹⁰ The clean Si(111)-7×7 surface was prepared *in situ* by standard flashing by dc current to 1200 °C and observed in STM after cooling to the desired

temperature. The STM tips were electrochemically etched from a polycrystalline W wire and treated *in situ* on a Pt(111) surface to ensure the metallic character of the tip.¹¹

The result of our STS measurements is a conventional density of states (DOS) obtained from the current-voltage characteristic $I_t(V_S)$ of the tunneling junction: $\text{DOS} = (dI_t/dV_S)/(I_t/V_S)$, where I_t is the tunneling current and V_S is the sample voltage with respect to the tip.¹² The energy of the electron states of the sample contributing to DOS is eV_S with respect to the sample bulk Fermi level. We measure the I_t and dI_t/dV_S simultaneously using a lock-in technique. For point STS spectra, we stabilize the STM feedback to I_t^0 , V_S^0 , switch it off, and measure the DOS as a function of V_S . We use the technique of continuously varying tip-sample separation s , $ds = ad|V_S|$. For the calculation of the point STS spectra, we use the broadening of the I_t/V_S by ΔV .¹² For spectroscopic imaging, we stabilize the STM feedback to I_t^0 , V_S^0 , switch it off, and measure the DOS as a function of (x, y) during scanning the tip at a plane parallel to the surface at $V_S = \text{const}$. $\text{DOS}(x, y)$ is calculated from the $dI_t/dV_S(x, y)$, $I_t(x, y)$, and V_S yielding a map where the DOS intensities are within $\pm 15\%$ of those obtained from the point STS measurements.¹³

In Fig. 1 we show point STS spectra of the Si(111)-7×7 surface measured at $T = 7 \text{ K}$ on rest atoms, center adatoms, and corner adatoms. We observe spectral features at $V_S = (-1.3, -0.9, -0.5, 1.2, 1.4, 1.6) \text{ V}$. The localization of the spectral features on the surface atoms is not perfect. We can, however, make an initial assignment of the spectral features to the surface atoms, where the respective DOS reaches a maximum. We, thus, assign the feature at $V_S = -1.3 \text{ V}$ to rest atoms (S_2), features at $V_S = (-0.9, -0.5, 1.4) \text{ V}$ to corner adatoms (S'_1, S_1, U_1), and at $V_S = (1.2, 1.6) \text{ V}$ to center adatoms (U'_1, U''_1). The features on rest atoms and corner adatoms have their analogs in previous investigations. We use the standard nomenclature for them.^{4,5} The features on center adatoms are observed for the first time and reveal the fine structure of the empty states in the adatom band. We derive their names from the U_1 .

We confirm the assignment of the spectral features by

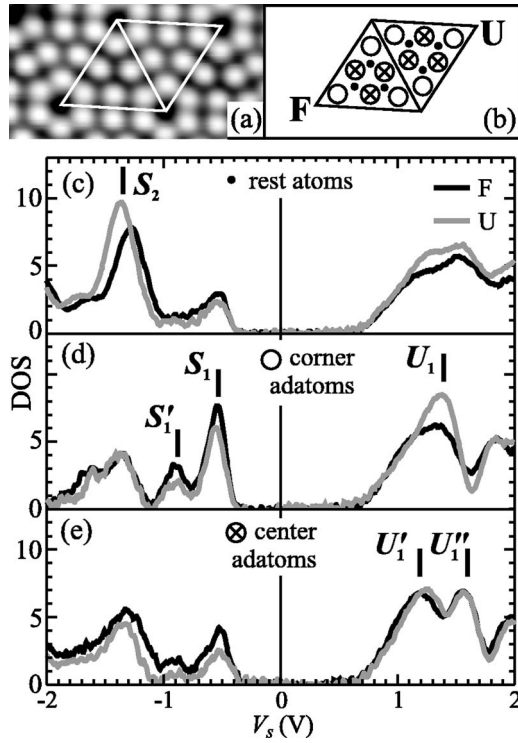


FIG. 1. (a) STM topography of the Si(111)- 7×7 surface unit cell. (b) Schematic of the surface atoms and orientation of the faulted (F) and unfaulted (U) half-unit cells. (c)–(e) STS spectra measured on the surface atoms at $T=7$ K and assignment of the Si(111)- 7×7 surface electronic features to rest atoms [S_2 , (c)], corner adatoms [S'_1 , S_1 , U_1 , (d)], and center adatoms [U'_1 , U''_1 , (e)]. Corner adatoms and center adatoms exhibit a distinctly different structure of the unoccupied states. $V_s^0=2$ V, $I_t^0=0.1$ nA, $a=0.4$ Å V^{-1} , $\Delta V=2$ V.

spectroscopic imaging. In Fig. 2, we show the wave functions (DOS maps) of surface electrons on Si(111)- 7×7 . From measurements at various V_s , we obtain an unambiguous assignment of the feature S_2 to rest atoms [Fig. 2(a)], S_1 and U_1 to corner adatoms [Figs. 2(b) and 2(c)], and U'_1 to center adatoms [Fig. 2(d)]. We note the pronounced splitting of the adatom electron states between the corner adatoms and center adatoms of the Si(111)- 7×7 surface [Figs. 2(b)–2(d)] that has not been observed in the previous measurements.^{2,14,15} Not shown are the STS images at $V_s=-0.9$ V (S'_1) that do not provide enough evidence for the assignment of the feature S'_1 to corner adatoms due to a high noise level, and the STS images at $V_s=1.2$ V (U'_1) that show the same DOS for corner and center adatoms.

In the following, we investigate the energy scale of our

LT STS measurements. The absolute values of the energies of the Si(111)- 7×7 surface electronic features measured at 7 K are higher compared to measurements by integral techniques^{4,5} or RT STS.^{2,14,15} Additionally, an apparent band gap opens around $V_s=0$ V [Figs. 1(c)–1(e)]. The shifts of the STS peaks and/or the changes in the measured band gap were observed in previous LT STS studies on semiconductors.^{6,7} They were assigned to a limited transport of the electrons between the surface and the bulk.⁷ A signature of the limited transport of electrons in the LT STS is a logarithmic shift of STS features away from $V_s=0$ V with increasing $|I_t^0|$.⁷ In Fig. 3(a), we show that such a shift appears for the empty state features in our LT STS measurements as well. Thus, our LT STS spectra are influenced by the limited transport of electrons.

Generally, the transport limitations in STS decrease with increasing temperature.^{6,7} We performed the measurements at increased temperature and show their results in Figs. 3(b)–3(d). We compare point STS spectra of faulted center and corner adatoms measured at 7 K (b), 77 K (c), and 297 K (d). We observe that all STS features shift toward $V_s=0$ V with increasing temperature and the apparent band gap disappears. At RT, we observe no significant dependence of the STS curves on I_t^0 , indicating that the limited electron transport does not influence the energy scale of the RT STS measurement. Moreover, we can still identify all spectral features in the RT spectra [Fig. 3(d)]. Thus, we can obtain true energies of the surface electronic states on the Si(111)- 7×7 surface from the fitting of point STS spectra measured at RT.

The point STS spectra measured at 77 and 297 K also yield additional information regarding the assignment of the features S'_1 and U'_1 to the surface adatoms. The peak S'_1 appears only in faulted corner adatom spectra measured at 77 K. We, thus, assign this feature to faulted corner adatoms (cf. Ref. 5). The peak U_1 of corner adatoms systematically shows a shoulder at an energy comparable to the energy of the peak U'_1 of center adatoms. Therefore, we assign the spectral feature U'_1 to both center and corner adatoms.

We summarize our findings regarding the structure of the adatom electron band of the Si(111)- 7×7 surface in Table I. The findings are in good agreement with previous studies of the Si(111)- 7×7 surface electronic structure.^{2,4,5,14,15} The combination of LT and RT STS allowed us to gain a more detailed insight: we identify new spectral features U'_1 and U''_1 in the unoccupied part of the adatom band and a pronounced splitting of adatom electron states between corner and center adatoms. Such splitting was predicted by a recent theoretical study that takes into account the mutual interactions of the surface electrons.¹⁶ However, this theory predicts that the

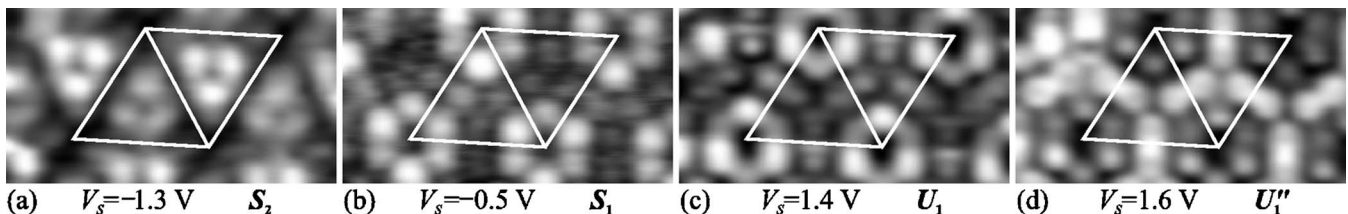


FIG. 2. Wave functions of the surface electrons measured at $T=7$ K (DOS maps). Maps show the spatial extent of the rest atom state [S_2 (a)], the occupied adatom state [S_1 (b)], and the unoccupied adatom states [U_1 (c) and U''_1 (d)]. The states U_1 and U''_1 belong to corner and center adatoms, respectively. $V_s^0=2$ V, $I_t^0=0.1$ nA. Figure orientation is the same as in Fig. 1(b).

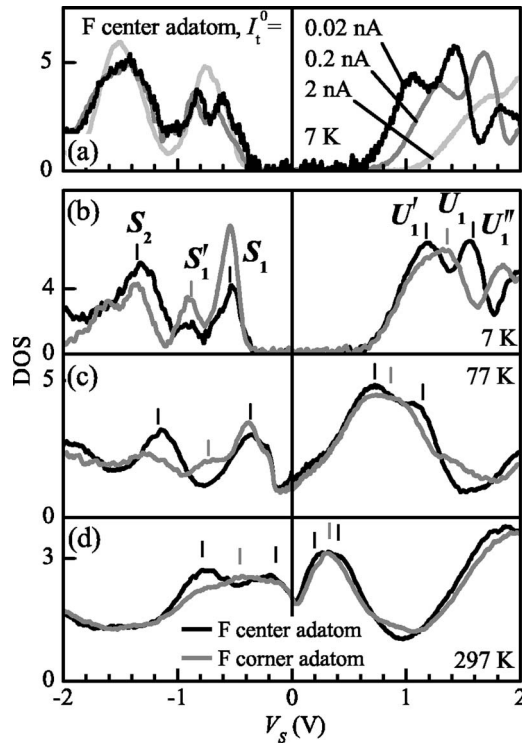


FIG. 3. (a) Dependence of the STS spectra on I_t^0 at $T=7$ K indicates that a limited transport of electrons influences the measurement. (b)–(d) Transport limitations decrease when the temperature increases [$T=7$, 77, and 297 K (RT) in (b), (c), and (d)]. Spectra do not depend on I_t^0 at RT allowing the energies of the rest atom state [S_2 (b)] and the adatom states [S'_1 – U''_1 , from left to right in (b)] to be determined from RT measurement (d), Table I.

energy of the center adatom state (U''_1) is close to 0 eV and below the energy of the unoccupied corner adatom state (U_1), which we do not observe. Our experimental results are closer to the structure of single-electron states calculated by *ab initio* methods¹⁷ that predict qualitative differences between the electron states of the corner and center adatoms.

Finally, we discuss the shifts of spectral features in our LT STS measurements in terms of the theory of LT nonequilibrium tunneling.⁷ Figure 4(a) shows the energy level schematic of nonequilibrium tunneling into the empty states of the highly *n*-doped Si(111)- 7×7 surface. Due to the electron transport problem between the surface and the bulk, the sur-

TABLE I. The structure of the adatom electron band of the Si(111)- 7×7 surface determined using LT and RT STS and STS imaging.

STS peak	Location	Energy at RT (eV)
S_2	Rest atoms	-0.78 ± 0.05
S'_1	Faulted corner adatoms	-0.45 ± 0.05
S_1	Corner adatoms	-0.14 ± 0.05
U'_1	Center and corner adatoms	0.20 ± 0.05
U_1	Corner adatoms	0.33 ± 0.05
U''_1	Center adatoms	0.41 ± 0.05

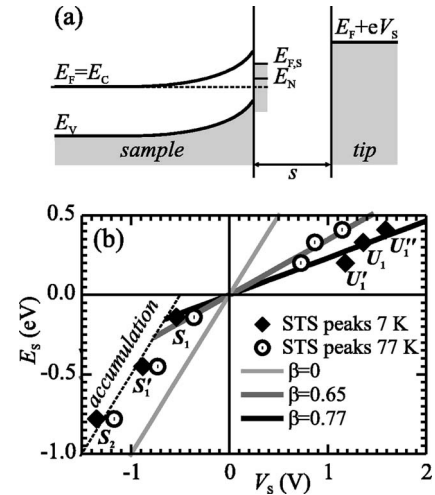


FIG. 4. (a) Energy level schematic of the nonequilibrium tunneling on Si(111)- 7×7 . (b) Plots of the true energy of STS peaks E_S as a function of V_S . Experimental data for 7 and 77 K exhibit a linear behavior $E_S=(1-\beta)eV_S$ for V_S where the Si(111) substrate is in depletion.

face accommodates an excess electric charge and the surface Fermi level $E_{F,S}$ shifts between the bulk Fermi level E_F and the tip Fermi level E_F+eV_S . The excess surface charge is, in turn, accommodated by shifting the $E_{F,S}$ with respect to the surface neutrality level E_N . The Si(111)- 7×7 surface has a high density of surface states resulting in strong surface Fermi level pinning.¹⁸ Therefore, accommodating the excess surface charge requires a small mutual shift of $E_{F,S}$ and E_N , $E_{F,S}\approx E_N$.¹⁹ Under such conditions, the true energy E_S of a measured surface STS feature will be shifted from E_F+eV_S by $E_{F,S}$, $E_S=E_F+eV_S-E_{F,S}$.

A relation of E_S to V_S can be found provided that the nonequilibrium response of $E_{F,S}$ to I_t and V_S is known. Obtaining the exact response would be a difficult task involving a detailed knowledge of the electron transport mechanisms between the surface and the bulk. Instead, we consider a simple model where $E_{F,S}$ is a linear function of V_S , $E_{F,S}=E_F+\beta eV_S$, and β is an effective measure of the surface nonequilibrium, $0\leq\beta<1$. Such an assumption yields $E_S=(1-\beta)eV_S$.

In Fig. 4(b), we show the plots of the true energy E_S as a function of the tunneling voltage V_S for the STS peaks measured at 7 K [Fig. 3(b)] and 77 K [Fig. 3(c)]. For E_S we take the energies of the peaks measured at RT (Table I). The dependence of E_S on V_S for the four peaks at the highest energies can be fitted by a line yielding $\beta_{7\text{ K}}=0.77$ and $\beta_{77\text{ K}}=0.65$. Thus, our simple model of the nonequilibrium response of $E_{F,S}$ holds for the STS measurements at higher energies [performed at $I_t^0=\text{const.}$, cf. Fig. 3(a)]. The behavior of the two peaks at the lowest energies differs qualitatively, because for $E_{F,S}\approx E_F-0.5$ eV the Si bulk reaches the flat band condition [dashed line in Fig. 4(b)] and the response to further accumulation of the surface charge by bulk band bending substantially decreases. Such an effect can be observed in Fig. 3(a), where the lower energy peaks do not respond to changes of I_t^0 by shifting.

We give the following explanation of the limited transport

of electrons between the Si(111)- 7×7 surface and bulk at LT. It has been shown that at RT the electrons tunneling into the empty surface states proceed to the bulk preferably by traveling *along* the surface to (defect) places, where the scattering into the bulk is easy.²⁰ Thus, the surface conductivity of the Si(111)- 7×7 surface helps the electrons to bypass the charge depletion layer that isolates the surface from the bulk. On the other hand, the Si(111)- 7×7 surface conductivity is thermally activated and vanishes at low temperatures.²¹ The easy transport channel is lost and the surface moves to nonequilibrium configuration where the bulk band bending changes until the tunneling between the surface and the bulk becomes effective.

In this paper, we combined LT and RT STS and spectroscopic imaging to obtain complete spatial and energetic information on the electronic structure of the Si(111)- 7×7 surface adatom band. We identified new spectral features in

the unoccupied part of the adatom band and a pronounced splitting of the adatom electron states between corner and center adatoms of the Si(111)- 7×7 reconstruction. We described the LT nonequilibrium tunneling on the Si(111)- 7×7 surface, which is characteristic of a surface with a high density of surface electron states at the Fermi level.

We gratefully acknowledge the illuminating discussions with Martin Wenderoth, Philipp Jaschinsky, and Vasily Cherepanov, the technical support from Helmut Stollwerk and Peter Coenen, and the careful reading of the manuscript by Janet Carter-Sigglow. The transport properties of our substrates were measured in the laboratory of Thomas Schäpers with the expert assistance of Vitaly Guzenko. This work was partially supported by Marie Curie Actions and by the Grant Agency of the Czech Republic (Contract No. GAČR 202/03/0792).

*Electronic address: b.voigtlaender@fz-juelich.de

¹G. Binnig, H. Rohrer, Ch. Gerber, and E. Weibel, Phys. Rev. Lett. **50**, 120 (1983).

²R. J. Hamers, R. M. Tromp, and J. E. Demuth, Phys. Rev. Lett. **56**, 1972 (1986).

³K. Takayanagi, Y. Tanishiro, M. Takahashi, and S. Takahashi, J. Vac. Sci. Technol. A **3**, 1502 (1985).

⁴F. J. Himpsel and Th. Fauster, J. Vac. Sci. Technol. A **2**, 815 (1984); R. I. G. Uhrberg, G. V. Hansson, J. M. Nicholls, P. E. S. Persson, and S. A. Flodström, Phys. Rev. B **31**, 3805 (1985); J. M. Nicholls and B. Reihl, *ibid.* **36**, 8071 (1987); R. Losio, K. N. Altmann, and F. J. Himpsel, *ibid.* **61**, 10845 (2000).

⁵R. I. G. Uhrberg, T. Kaurila, and Y.-C. Chao, Phys. Rev. B **58**, R1730 (1998).

⁶G. Dujardin, A. J. Mayne, and F. Rose, Phys. Rev. Lett. **89**, 036802 (2002); T. Yokoyama and K. Takayanagi, Phys. Rev. B **61**, R5078 (2000); R. M. Feenstra, G. Meyer, and K. H. Rieder, *ibid.* **69**, 081309 (2004).

⁷R. M. Feenstra, S. Gaan, G. Meyer, and K. H. Rieder, Phys. Rev. B **71**, 125316 (2005).

⁸SPS-CreaTec GmbH, Erligheim, Germany.

⁹I. Ošt'ádal, P. Kocán, P. Sobotík, and J. Pudl, Phys. Rev. Lett. **95**, 146101 (2005).

¹⁰The transport properties of our samples were measured by LT van der Pauw and Hall measurements.

¹¹R. M. Feenstra, G. Meyer, F. Moresco, and K.-H. Rieder, Phys. Rev. B **64**, 081306(R) (2001).

¹²J. A. Stroscio and R. M. Feenstra, in *Scanning Tunneling Microscopy*, edited by J. A. Stroscio and W. J. Kaiser (Academic, San Diego, 1993).

¹³Our method differs from current imaging tunneling spectroscopy (CITS, Ref. 2) that generally does not yield DOS maps, see Ref. 12.

¹⁴R. Wolkow and Ph. Avouris, Phys. Rev. Lett. **60**, 1049 (1988).

¹⁵R. Negishi and Y. Shigeta, Surf. Sci. **507**, 582 (2002).

¹⁶J. Ortega, F. Flores, and A. L. Yeyati, Phys. Rev. B **58**, 4584 (1998).

¹⁷M. Fujita, H. Nagoshi, and A. Yoshimori, Surf. Sci. **242**, 229 (1991); K. D. Brommer, M. Galván, A. Dal Pino, Jr., and J. D. Joannopoulos, Surf. Sci. **314**, 57 (1994).

¹⁸J. Viernow, M. Henzler, W. L. O'Brien, F. K. Men, F. M. Leible, D. Y. Petrovykh, J. L. Lin, and F. J. Himpsel, Phys. Rev. B **57**, 2321 (1998).

¹⁹An estimate based on a model from Ref. 7 for an Si substrate doped to $1.6\times 10^{19}\text{ cm}^{-3}$, tip-sample distance 6 Å, Pt tip, planar geometry, Schottky depletion layer, and average density of Si(111)- 7×7 surface states $\sigma'=7.7\times 10^{14}\text{ cm}^{-2}\text{ eV}^{-1}$ yields $|E_{F,S}-E_N|<20\text{ meV}$ for $|V_S|<2\text{ V}$ and $E_F\leq E_{F,S}<E_F+eV_S$.

²⁰S. Heike, S. Watanabe, Y. Wada, and T. Hashizume, Phys. Rev. Lett. **81**, 890 (1998); Jpn. J. Appl. Phys., Part 1 **38**, 3866 (1999).

²¹T. Tanikawa, K. Yoo, I. Matsuda, S. Hasegawa, and Y. Hasegawa, Phys. Rev. B **68**, 113303 (2003).